Transcripts with codons that trigger the P-site tRNA–mediated mRNA decay are enriched with optimal codons

Rodolfo L. Carneiro and Fernando L. Palhano*
Programa de Biologia Estrutural, Instituto de Bioquímica Médica Leopoldo de Meis, Universidade Federal do Rio de Janeiro, Rio de Janeiro, RJ, 21941-902, Brazil.

* To whom correspondence should be addressed: Tel.: +55 21 3938-6761; Email: palhano@bioqmed.ufrj.br

Abstract

Synonymous codon usage is a major determinant of mRNA half-life in yeast, functioning as a second layer of genetic information during translation. In this system, the CCR4-NOT complex plays a key role by interacting with the ribosome when both its A and E sites are vacant—a state that typically occurs when a non-optimal codon, i.e., one with low tRNA availability, occupies the A site. The complex then recruits the mRNA decay machinery, leading to shorter half-lives for transcripts enriched in non-optimal codons. In humans, the extent to which codon usage affects mRNA stability remains unclear. Recent studies have shown that CCR4-NOT recruitment in humans shares some similarities with yeast but also exhibits significant mechanistic differences. In particular, CCR4-NOT binding depends on the presence of specific arginine codons —CGG, CGA, or AGG—at the P site of the ribosome, a process termed P-site tRNA-mediated decay (PTMD). PTMD also requires slow decoding at the A site, enabling E-site vacancy and subsequent CCR4-NOT recruitment by CNOT3. Using high-throughput analyses of public datasets, we investigated how human transcripts enriched in PTMD codons differ from the rest of the transcriptome in terms of codon optimality, mRNA half-life, and protein abundance. We find that PTMD-target codons are predominantly present in transcripts with overall optimal codon usage and longer half-lives. This suggests that, in contrast to yeast, PTMD in humans preferentially shortens the half-lives of otherwise stable transcripts, rather than contributing to the degradation of inherently unstable ones.

Introduction

Precise control of messenger RNA (mRNA) turnover is a key regulatory mechanism in numerous cellular processes. Some of these are inherent to mRNA function—for instance, transcripts with longer half-lives tend to accumulate in the cytoplasm and are translated into highly expressed proteins. Additionally, mRNA decay regulation has been linked to the immune response (Hwang et al., 2020), responses to mRNA damage (Frischmeyer et al., 2002; Wurtmann & Wolin, 2009; Yan et al., 2019; Klauer & van Hoof, 2012), and cell cycle progression and differentiation (Yu et al., 2016; Bazzini et al., 2016; Mishima & Tomari, 2016). Various molecular machineries regulate mRNA decay, acting either globally or targeting specific motifs in transcript sequences (Dowdle & Lykke-Andersen, 2025).

The canonical pathway of mRNA degradation begins with deadenylation at the 3′ end by the Pan2–Pan3 and CCR4–NOT complexes (Passmore & Coller, 2022; Wolf & Passmore, 2014), followed by decapping at the 5′ end by the Dcp1–Dcp2 complex. Once the mRNA ends are exposed, the exonuclease Xrn1 degrades the transcript in the 5′ to 3′ direction (Jinek, Coyle, & Doudna, 2011), while the Ski complex facilitates 3′ to 5′ degradation (Johnson & Kolodner, 1995; Anderson & Parker, 1998).

Although this canonical pathway is largely translation-independent, increasing attention has been given to translation-dependent regulation of mRNA stability, especially through synonymous codon usage. Despite the degeneracy of the genetic code, synonymous codons can influence mRNA half-life and protein expression (Presnyak et al., 2015).

Presnyak and colleagues demonstrated that codon optimality correlates with mRNA stability. Codon optimality reflects how likely a codon is, on average, to be efficiently decoded by its cognate tRNA at the ribosomal A-site. This relationship is mediated by the CCR4–NOT complex (Webster et al., 2018; Buschauer et al., 2020). In yeast, the Not5 subunit of the CCR4–NOT complex interacts with the ribosomal E-site when both the A and E sites are unoccupied—a ribosome conformation that arises during slow decoding of non-optimal codons. This interaction promotes recruitment of the decapping factor Dhh1 and subsequent mRNA decay (Radhakrishnan et al., 2016; Buschauer et al., 2020).

While this codon optimality–mRNA stability link is best characterized in yeast, it appears to be conserved across multiple species, including *Escherichia coli* (Böel et al., 2016), zebrafish (Bazzini et al., 2016; Mishima & Tomari, 2016), *Trypanosoma brucei* (Nascimento et al., 2018; Jeacock, Faria, & Horn, 2018), *Drosophila melanogaster* (Burow et al., 2018), and humans (Wu et al., 2019; Forrest et al., 2020).

In humans, however, the molecular mechanisms differ in key ways. A recent study revealed that CNOT3, the human homolog of yeast Not5, targets transcripts based on the structure of the tRNA occupying the ribosomal P-site (Zhu et al., 2024). Using ribosome footprint profiling in HEK293T cells, the authors showed that CNOT3 preferentially associates with ribosomes translating three specific arginine codons—CGA, CGG, and AGG—when both the A and E sites are vacant. This process, termed P-site tRNA-mediated decay (PTMD), requires both the presence of one of these codons in the P-site and slow decoding at the A-site to enable E-site vacancy and CCR4–NOT recruitment. Knockout of CNOT3 stabilizes numerous transcripts enriched in these codons, supporting its role in mRNA destabilization.

Despite these findings, it remains unclear whether non-optimal codons (i.e., those with low cognate tRNA levels) are the principal determinants of translation-dependent mRNA decay in humans—as has been widely demonstrated in yeast—or whether other features such as amino acid identity also play significant roles (Forrest et al., 2020).

In this study, we investigate the genomic landscape of PTMD regulation by analyzing genes enriched in CGA, CGG, and AGG codons. Using datasets from Zhu et al. (2024) and additional sources, we examine how PTMD-targeted transcripts differ in codon optimality, mRNA stability, and protein abundance. Our results show that PTMD-target codons are primarily found in transcripts with long half-lives and high codon optimality, whereas unstable transcripts and those rich in non-optimal codons tend to lack PTMD codons. These findings suggest that PTMD serves as a mechanism to reduce the half-lives of otherwise stable transcripts, rather than mediating decay of inherently unstable mRNAs.

Results

PTMD target codons tend to be followed by optimal codons and are associated with stable mRNA transcripts

With CNOT3 being the human homolog of Not5 in yeast, it was expected that its regulatory properties would be associated with codon optimality at the A-site. The model proposed by Mendell's group suggests maximal recruitment of the CCR4-NOT complex occurs under the combination of an A-site occupied by a rare codon, leading to simultaneous A- and E-site vacancies; and a CGG, CGA, or AGG codon at the P-site (Zhu et al., 2024).

The experimental evidence supporting this model is the observed correlation between A-site dwell time and CNOT3 association when the P-site is occupied by a CGG, CGA, or AGG codon (Zhu et al., 2024). To further investigate this model, we developed an algorithm to scan all human transcript sequences for CGG, CGA, or AGG codons and assess the optimality of the codons immediately following them.

To quantify codon optimality, we used the tRNA Adaptation Index (tAI), which reflects the abundance of each tRNA in the genome and the strength of codon-anticodon pairing (dos Reis, Savva, & Wernisch, 2004). Interestingly, we found that CGA, CGG, and AGG codons are less frequently followed by non-optimal codons than would be expected based on overall codon distribution (Fig. 1A and 1B). These findings suggest that transcripts containing PTMD codons tend to avoid maximal CCR4-NOT recruitment by favoring optimal codons (high tAI) in the A-site when a PTMD codon occupies the P-site during translation.

Building on this observation, we tested whether transcripts enriched in PTMD codons also exhibit increased mRNA stability. Following the methodology used by Mendell's group, we calculated a PTMD score for each transcript, weighting the CGG, CGA, and AGG codons by their enrichment in the P-site of CNOT3-associated ribosomes and normalizing by the total number of codons in the ORF.

PTMD scores showed a positive Spearman correlation with codon optimality metrics, including tAI, GC content, and average Codon Stability Coefficient (CSCg), a measure of the correlation between individual codons and mRNA half-life (Presnyak et al., 2015; Carneiro et al., 2019) (Fig. 1E). Surprisingly, the correlation between PTMD score and CSCg was even stronger than that with mRNA half-life itself. In contrast, protein abundance—while positively correlated with mRNA half-life—did not show a significant correlation with PTMD score (Fig. 1F).

We then selected the top 1,000 transcripts with the highest PTMD scores from the 7,639 transcripts for which mRNA half-life data were available (Zhu et al., 2024). These transcripts had significantly higher codon optimality values (Figs. 1C and 1D), supporting our hypothesis that transcripts enriched in CGG, CGA, and AGG codons also tend to have more optimal codon usage overall.

Given that PTMD-rich transcripts tend to be enriched in optimal codons, we next evaluated whether they also tend to have longer mRNA half-lives. Indeed, these transcripts had significantly longer half-lives compared to the rest of the transcriptome (Fig. 2B). Conversely, the genes showing the greatest increase in mRNA stability upon CNOT3 knockout also had higher PTMD scores (Fig. S1B).

These findings do not imply that PTMD has no role in destabilizing mRNAs. Rather, when comparing mRNA half-lives in CNOT3-knockout (sgCNOT3) cells, we observed even greater stability of these transcripts (Fig. 2C, 2D; Supplemental Fig. 1C, 1D). In other words, the PTMD machinery preferentially targets transcripts with high codon optimality, thereby reducing their mRNA half-life.

The effect of codon optimality in the A-site neighbor PTMD codons on CNOT3-mediated mRNA decay

The fact that the PTMD machinery preferentially targets transcripts with optimal codons (Figs. 1C and 1E) does not invalidate the model proposed by Mendell's group for maximal recruitment of the CCR4-NOT complex upon translation of rare codons. To further test this model, we asked whether non-optimal codons at the A-site, adjacent to PTMD codons, promote CNOT3-mediated mRNA decay.

To address this question, we stratified the top 1,000 transcripts with the highest PTMD scores into two groups: one consisting of the 500 transcripts in which the codon following AGG, CGA, or CGG had the highest tAI (most optimal A-site codons), and the other with the 500 transcripts with the lowest tAI (least optimal A-site codons).

Surprisingly, among high-PTMD score transcripts, those with the most optimal A-site codons—i.e., lowest dwell time and highest tAI—exhibited the largest increases in mRNA half-life upon CNOT3 knockout (Figs. 3A and 3B). This effect was not observed in transcripts with low PTMD scores (Figs. 3C and 3D). Importantly, this effect cannot be attributed to a higher abundance of AGG, CGA, or CGG codons in transcripts with optimal A-site codons, since there was no statistically significant mRNA half-life variance between optimal and non-optimal codons within the PTMD group (Supplemental Fig. S2 A and B).

While our results indicate a relationship between A-site codon optimality and PTMD-mediated decay, CNOT3's effects on mRNA half-life are not exclusively dependent on AGG, CGA, or CGG codons or A-site optimality (Fig. 4), as expected, given the broad regulatory role of the CCR4-NOT complex on mRNA turnover (Yi et al., 2018; Raisch & Valkov, 2022; Collart, 2016; Du et al., 2016; Enwerem et al., 2021; Hosoda et al., 2011; Ogami et al., 2014). Cluster analysis further supported this view: transcripts with the highest PTMD scores and lowest A-site tAI values did not overlap with those that showed the greatest increase in mRNA half-life upon CNOT3 knockout (Fig. 4).

Taken together, these results suggest no apparent effect of CNOT3-mediated mRNA decay on transcripts enriched in PTMD codons followed by non-optimal codons (Fig. 3). However, this does not contradict Mendell's model of PTMD-mediated CCR4-NOT recruitment. Rather, it implies that additional factors likely modulate the decay of transcripts containing PTMD codons.

A valuable next step would be to assess the half-life of reporter constructs enriched in PTMD codons, flanked by either optimal or non-optimal codons, to experimentally test the role of A-site codon identity in CNOT3-dependent decay.

Protein abundance is coupled to codon optimality independently of the effects of PTMD on mRNA half-life.

Codon optimality is a well-established determinant of both mRNA stability and protein expression across diverse species, particularly in yeast (Gustafsson, Govindarajan, & Minshull, 2004; Presnyak et al., 2015; Carneiro, Requião, Rossetto, Domitrovic, & Palhano, 2019). The central hypothesis underlying this coupling is that codons corresponding to low-abundance tRNAs promote transcript destabilization, resulting in reduced mRNA levels and lower protein synthesis.

Given that transcripts with high PTMD scores are enriched in optimal codons, which in turn influence several other features such as mRNA stability and protein output, we sought to disentangle the effects of PTMD codon enrichment from codon optimality. To do this, we reorganized our dataset into two groups: one containing transcripts with high PTMD scores and another with low PTMD scores. From these, we selected 500 transcripts from each group such that both sets shared a similar distribution of mRNA half-lives (Fig. 5A). This allowed us to compare other parameters—such as codon optimality (Fig. 5B), mRNA half-life under CNOT3 knockout conditions (Fig. 5C), and protein abundance (Fig. 5D)—in transcript sets that were matched for mRNA stability but differed in PTMD codon content.

Despite having comparable mRNA half-lives, transcripts with high PTMD scores exhibited significantly higher codon optimality (Fig. 5B) and longer half-lives upon CNOT3 knockout (Fig. 5C). Although transcripts with high PTMD scores exhibited a trend toward higher protein abundance (Fig. 5D), this difference was not statistically significant, indicating that PTMD codon enrichment does not appear to affect protein output in a consistent manner other than by mRNA decay.

To further test whether codon optimality was a confounding factor in our earlier analyses, we repeated the comparison using a different strategy: this time, we selected a control group of transcripts with similar tAI distributions to the high PTMD score group, enabling a comparison of transcripts with matched codon optimality. In this context, transcripts with high PTMD scores still displayed longer mRNA half-lives (Fig. 5E), suggesting that mechanisms independent of codon bias contribute to the enhanced stability of these transcripts. This effect was amplified under CNOT3 knockout conditions (Fig. 5G), further supporting the involvement of CCR4-NOT in regulating these transcripts. Interestingly, no statistically significant difference in protein abundance was observed between the two groups when codon optimality was matched (Figs. 5H and 5L).

Discussion

mRNA half-life correlation to codon optimality is conserved across various eukaryotic species, from yeast to humans. Nevertheless, PTMD via the CCR4-NOT complex operates differently in humans compared to yeast.

In yeast, the Not5 component of the CCR4-NOT complex targets non-optimal codons in the A-site. Codons with low tRNA availability are translated more slowly due to delayed codon-anticodon pairing, which promotes a ribosomal conformation with both the E-site and A-site vacant—this conformation is required for Not5 binding. Upon

binding, Not5 recruits the mRNA decay machinery, resulting in shorter half-lives for transcripts enriched in non-optimal codons.

Conversely, in humans, CNOT3—the homolog of Not5—preferentially targets specific codons in the P-site, particularly the AGG, CGA, and CGG codons of arginine. Although codon optimality is a major determinant of mRNA stability in yeast, its contribution to mRNA half-life in humans is less well understood. Bazzini and colleagues demonstrated that codon optimality is a major factor in human mRNA stability, independently of the poly-A tail (Wu et al., 2019). In contrast, Coller and colleagues highlighted the role of amino acid identity, in addition to codon bias, in mRNA regulation (Forrest et al., 2020).

We observed that genes enriched in AGG, CGA, and CGG arginine codons displayed characteristics associated with optimized transcripts, particularly in terms of the protein/mRNA ratio (Figs. 1 and 2). One possible explanation for this apparent discrepancy is the existence of a threshold number of PTMD codons required to recruit the CCR4-NOT complex. The minimal number of PTMD codons per transcript necessary to trigger mRNA degradation remains unknown. Mendell's group used a reporter containing 42 tripeptides centered on a PTMD arginine codon to demonstrate accelerated CNOT3-mediated mRNA decay (Zhu et al., 2024). Interestingly, only 20 human genes closely resemble this reporter, containing at least 14 PTMD codons within a 42-codon window (data not shown). The extent to which PTMD contributes to global mRNA half-life regulation and the evolutionary basis for its specificity toward a subset of arginine codons remain to be elucidated.

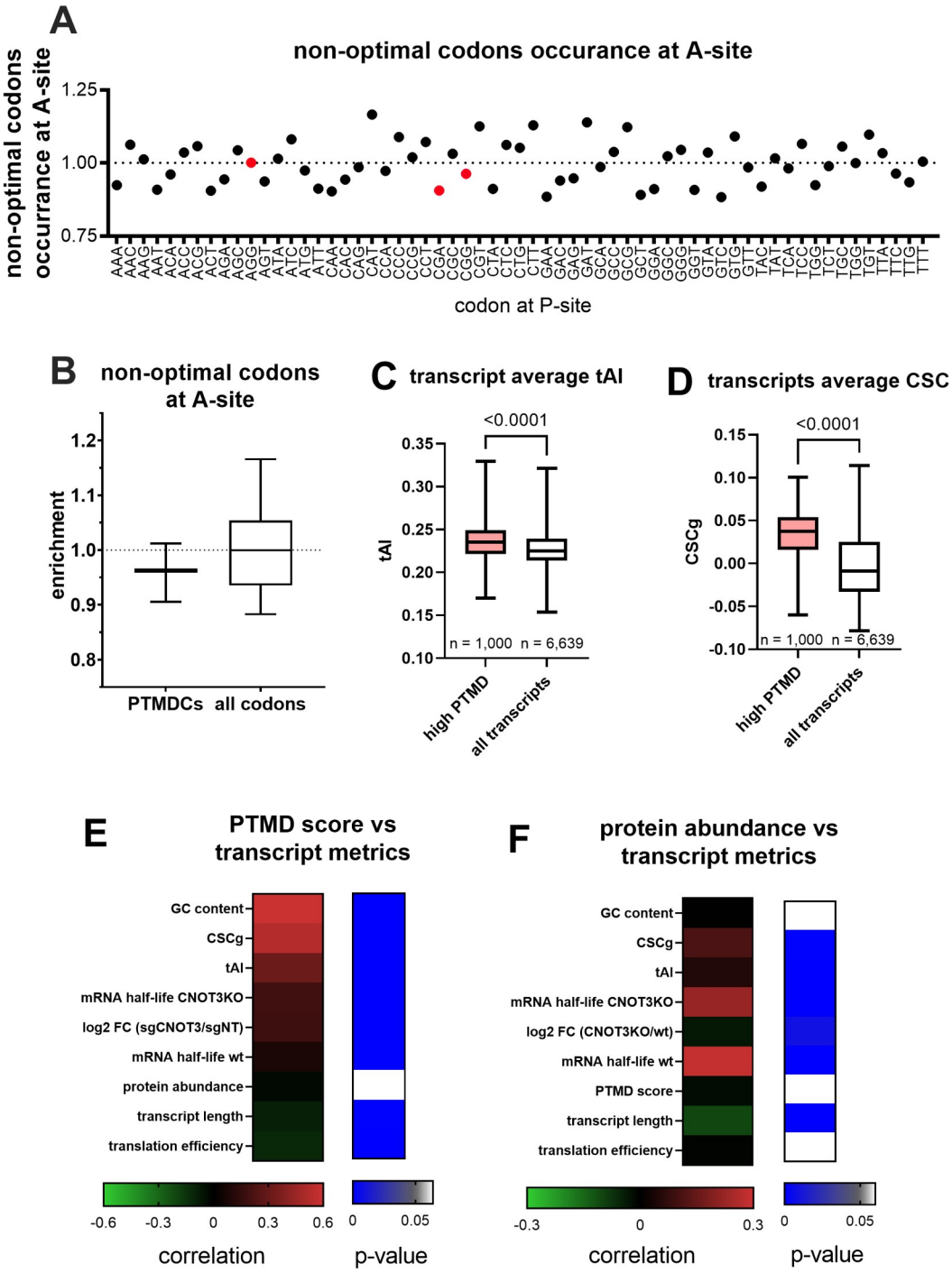

Figure 1. Comparisons of PTMD score and optimality metrics. (A) Comparison of non-optimal codon occurrence in the A-site (Y) after each codon in the P-site (X) genome. The full coding sequence of each gene was counted once. **(B)** It is the same as (A) but grouped in PTMD target codons and non-PTMD target codons. **(C)** Average of the tRNA adaptation index for each transcript among the transcripts rich in PTMD target codons vs the rest of the genome. **(D)** Average of the Codon Stability Coefficient for each transcript among the transcripts rich in PTMD target codons vs the rest of the genome. **(E)** Pearson's correlation index between PTMD score and other optimality metrics. **(F)** Pearson's correlation index between protein abundance and other optimality metrics.

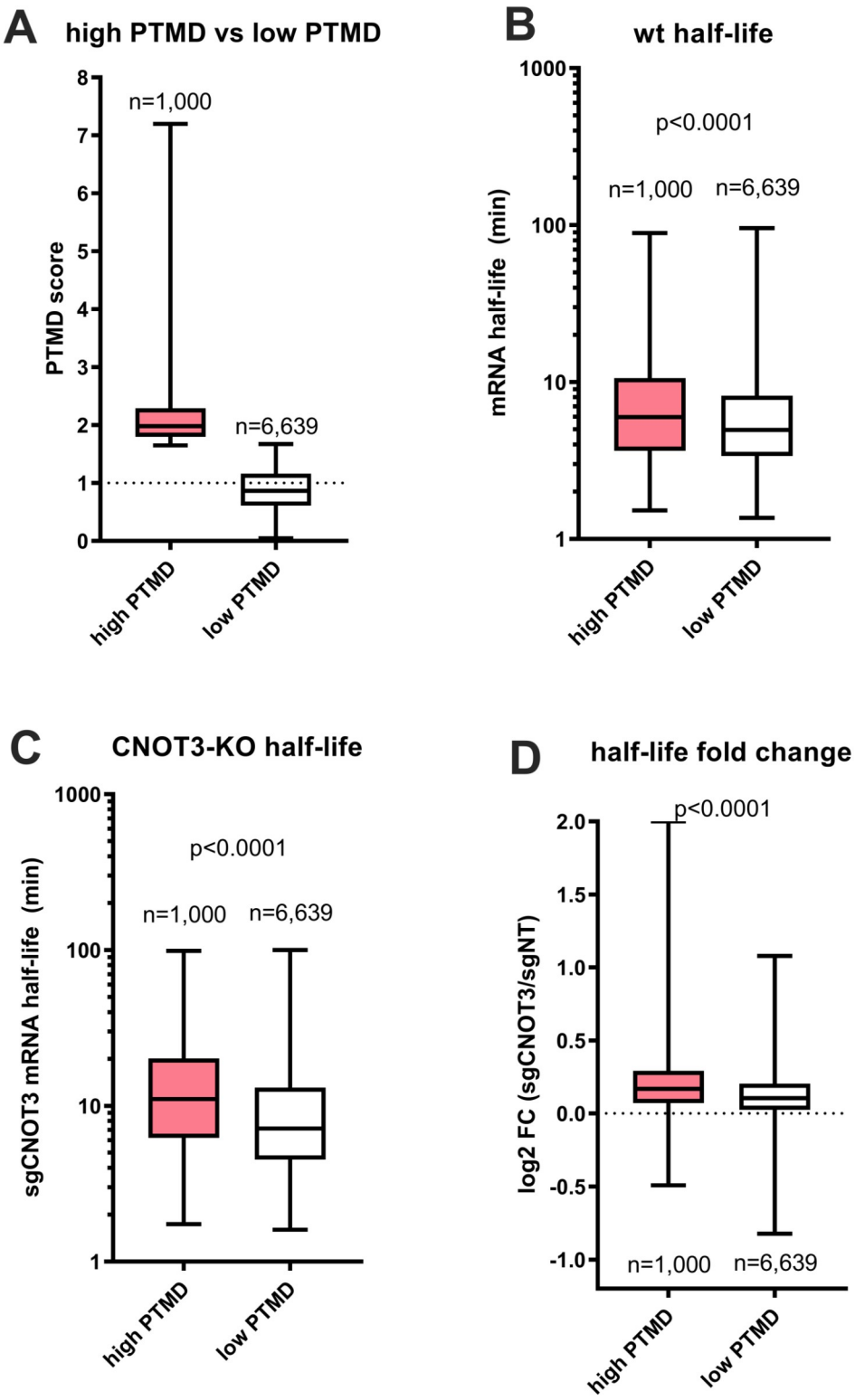

Figure 2. Comparison of PTMD score and transcripts rich in AGG, CGA, and CGG with other metrics. (A) Transcripts with high PTMD scores and other transcripts were split by their PTMD scores. **(B)** mRNA half-life of transcripts with high PTMD score compared to mRNA half-life of the remaining transcripts in wild-type cells. **(C)** mRNA half-life of transcripts with high PTMD score compared to mRNA half-life of the remaining transcripts in CNOT3-knockout cells. **(D)** Log2 of the mRNA half-life fold change between CNOT3-knockout cells and wild-type cells. p-values given by Kolmogorov-Smirnov test

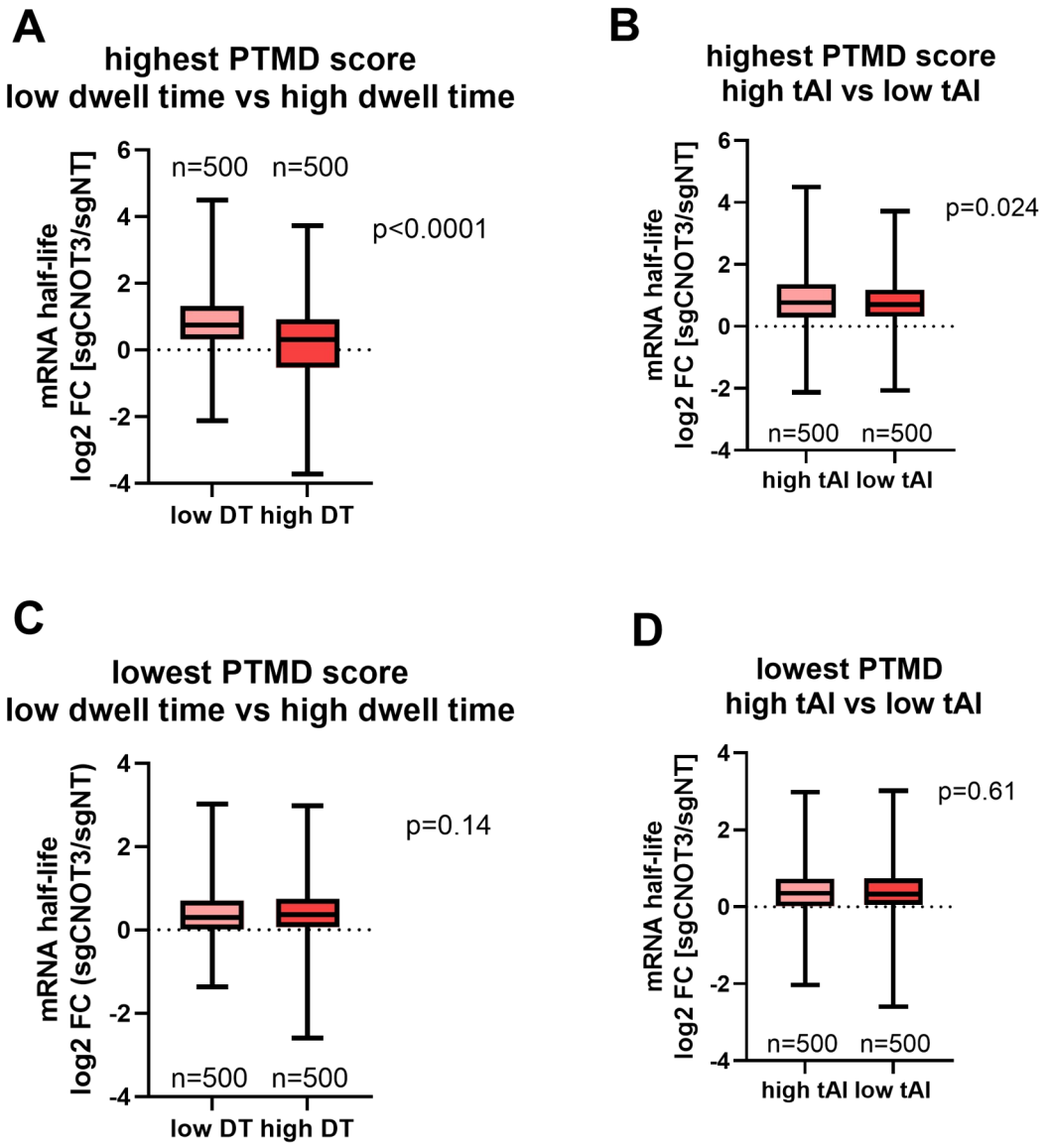

Figure 3. mRNA half-life changes due to CNOT3 recruitment on transcripts with high PTMD score, with different codon optimalities on the A-site (A) mRNA half-life fold change (sgCNOT3/sgNT) of transcripts with high PTMD score comparing the lowest dwell time in the A-site after CGA, CGG or AGG vs transcripts with the highest dwell time in the A-site after CGA, CGG or AGG. **(B)** Similar to panel A, this time, using the metric tAi at A site to split the two groups **(C, D)** Same analysis as (A) and (B), but with the 1,000 transcripts with the lowest PTMD score. Dwell time and tAI values for each transcript are the median of the dwell time of the codons following CGA, CGG, or AGG on those transcripts. p-values given by Kolmogorov-Smirnov test.

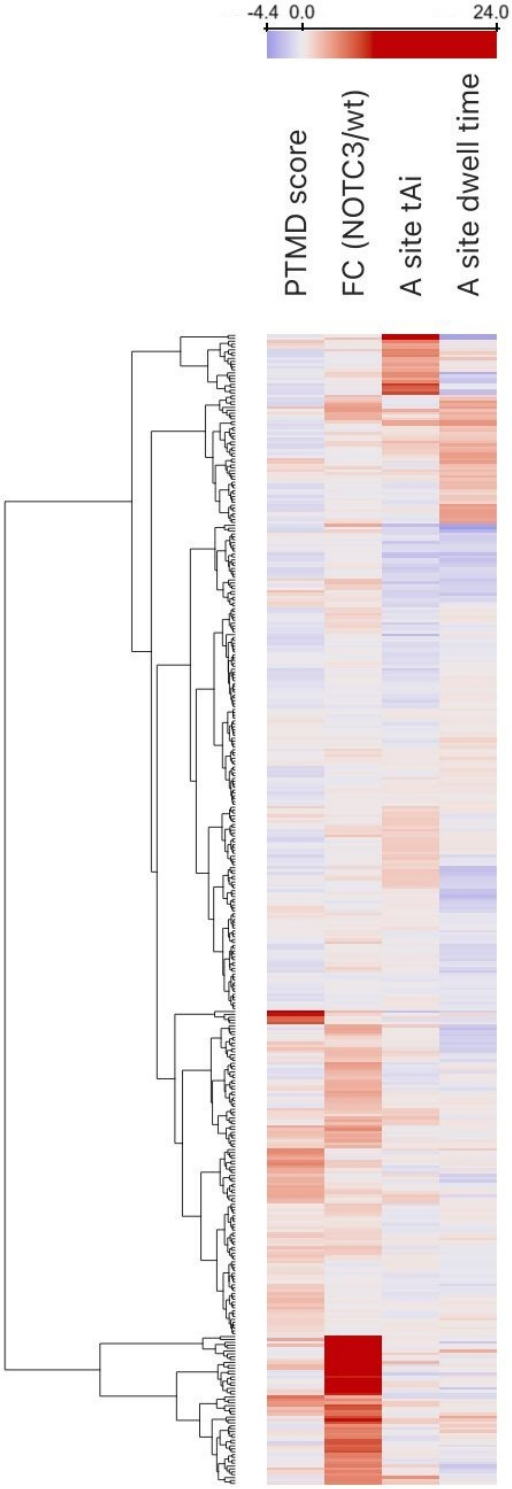

Figure 4. Cluster Analysis of PTMD score, mRNA half-life change after CNOT3 knockout, and A-site tAI or dwell time. Each 7,639 transcripts was grouped in one of 400 groups (k means), according to their similarity on the four metrics. Each line represents the average values of the transcripts in the group. The number of transcripts in each group may vary. The Values were normalized using Z-scores for each variable.

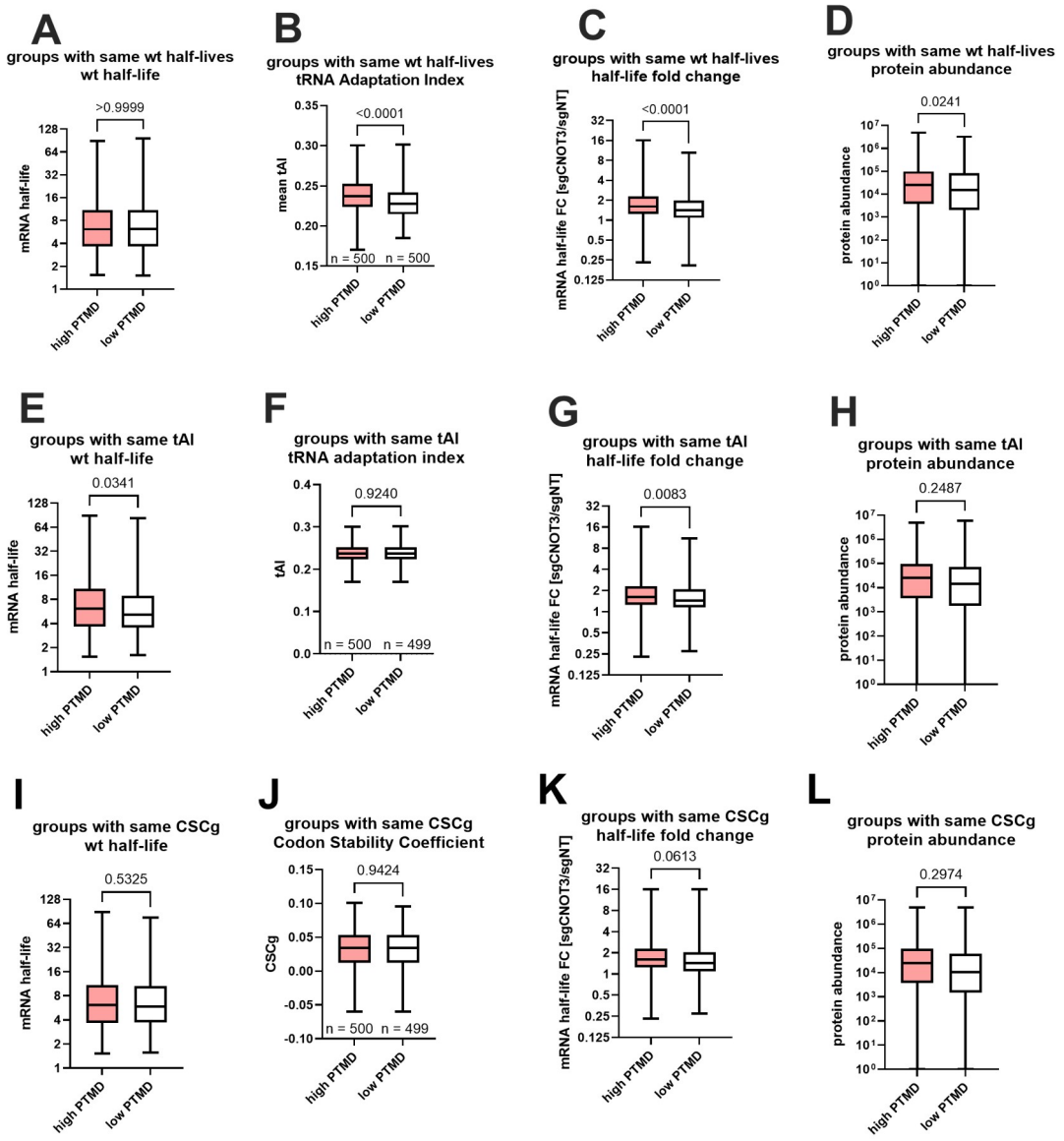

Figure 5. Effect of PTMD score in a group of transcripts with similar mRNA half-life, tAi or CSCg (A-D) Two groups of transcripts were chosen, one with the highest PTMD scores and the other with lower PTMD scores but with the same mRNA half-live distribution as the first group. The transcripts in each group are the same in figures from A to D. **(E-H).** The group with the highest PTMD scores remains the same. A new group of transcripts with similar tRNA Adaptation Index as the first, but with low PTMD scores was used in panels from E to H. **(I-L)** The same rearrangement was done, but now with CSC instead of tAI. **(A, E, I)** mRNA half-lives of each group on wt cells. **(B, F, J)** Codon optimality of each group. **(C, G, K)** Fold change between wt mRNA half-life and mRNA half-life on CNOT3-KO cells of each group. **(D, H, L)** Protein abundance in each group. Each group has 500 transcripts.

Methods

Data sources

Coding sequences (CDS) and gene annotations for *Homo sapiens* GRCh38 were downloaded from Ensembl. Transcripts were filtered to include only those with lengths divisible by three and ending with a canonical stop codon. To avoid redundancy and overrepresentation of genes with multiple isoforms, only the longest transcript per gene was retained. Of the 23,151 genes in the dataset, 17,324 (74.8%) had multiple annotated transcripts, with an average of 5.5 transcripts per gene. The selected longest transcripts had a mean length of 564 codons and an average PTMD score of 0.193. In contrast, the discarded transcripts had a mean length of 409 codons and an average PTMD score of 0.196.

Codon optimality metrics

The tRNA adaptation index (tAI) values used in this study were obtained from Forrest et al. (2020) and are the same as those used by Mendell's group (Zhu et al., 2024). Codon Stability Coefficients (CSC) were calculated based on mRNA half-life data from the same study. In CRISPR-based experiments, *sgCNOT3* refers to single guide RNAs targeting the *CNOT3* gene, while *sgNT* represents non-targeting control guides. Dwell time values shown in Figure 2E correspond to the translation elongation times assigned to each of the 61 sense codons, as reported by Narula et al. (2019).

Codon occurrence calculations

Non-optimal codons were arbitrarily defined as those with a tAI lower than the median of the codons, i.e., the 30 codons with the lowest tAI values. In Figure 1A, the "non-optimal codon occurrence" was calculated as the ratio between the frequency of non-optimal codons following a given codon by the frequency of non-optimal codons in the genome:

$$O_i = \frac{F_i}{F_{genome}}$$

Where O_i is the occurrence of non-optimal codons following the codon I, F_i is the frequency in which non-optimal codons are found following the codon I, and F_{genome} is the frequency in which non-optimal codons appear in the genome. Decomposing the frequencies, the same equation can also be written as:

$$O_i = \frac{\frac{N_i^{non-optimal}}{N_i}}{\frac{N^{non-optimal}}{N}}$$

Where O_i is the occurrence of non-optimal codons following the codon i, $N_i^{on\text{-}optimal}$ is the number of occurrences of non-optimal codons following the codon i, N_i is the number of occurrences of codon i in the genome, $N^{non\text{-}optimal}$ is the number of occurrences of non-optimal codons in the genome, and N is the number of codons in the genome.

The data used for Figs. 1 A and B is available in Supplemental Table 1.

PTMD score

The PTMD score used in Figures 2 and 4 was calculated based on how much the codons CGA, CGG, and AGG promote the recruitment of PTMD. These values were

derived from the data from Mendell's group of the codon occurrence on selective ribo-seq for CNOT3 compared to standard ribo-seq (Zhu et al., 2024).

The PTMD score of a transcript was defined as the occurrence of each of the PTMD target codons multiplied by their occurrence values as described above and divided by the transcript length in codons, following the equation:

$$score = \frac{\sum_i \left(N_i \cdot O_i \right)}{L}$$

Where N_i is the occurrence of the codon i, O_i is the occurrence of the codon i, and L is the transcript length in codons.

Search for PTMD codons and A-site codons following the PTMD codons

To identify transcripts containing PTMD target codons (AGG, CGA, or CGG) and the codons that appear in the A-site immediately after these PTMD codons occupy the P-site, we implemented a Python script that scans each coding sequence in our human transcriptome library. For every in-frame codon, the subsequent codon was considered to occupy the A-site relative to that P-site codon. In Figure 3, the dwell time and tAI values represent the median values of codons found in the A-site following each occurrence of AGG, CGA, or CGG. The median was chosen as the primary measure of central tendency due to the typically low frequency of PTMD codons per transcript, which can make the mean sensitive to outliers.

The data used for Fig. 1 C to F, and Figs 2 to 5 is available in Supplemental Table 2.

Definition of groups of transcripts with similar half-lives, tAI, and CSCg as the high-PTMD score group

In Figure 5, we selected a group of 500 transcripts with the highest PTMD scores after filtering out transcripts with missing protein abundance data. To generate a comparison group with low PTMD scores but a similar mRNA half-life distribution, we excluded the 1,000 transcripts with the highest PTMD scores and removed any with missing protein abundance values. Then, for each transcript in the high-PTMD group, we selected the transcript with the closest mRNA half-life from the remaining pool to create a low-PTMD group matched by half-life. This matching strategy ensures that differences between the groups are not attributable to mRNA half-life bias.

Similarly, we constructed comparison groups matched by tAI and CSCg values. These were formed by selecting, for each high-PTMD transcript, the transcript with the nearest tAI or CSCg value among those with low PTMD scores. In each case, the goal was to isolate the impact of PTMD score by controlling for a specific parameter of interest.

Acknowledgments

We thank Joshua Mendell and Xiaoqiang Zhu for kindly sharing their data with us. We are also grateful to Janaina de Freitas Nascimento and Xiaoqiang Zhu for the critical reading of our manuscript.

Funding
This work was supported by Conselho Nacional de Desenvolvimento Científico e Tecnológico (CNPq), Fundação de Amparo a Pesquisa do Estado do Rio de Janeiro (FAPERJ) and Coordenação de Aperfeiçoamento de Pessoal de Nível Superior (CAPES).

Conflict of interest
The authors declare that they have no conflicts of interest with the contents of this article.

Supplemental data
Supplemental data for this article can be accessed on the publisher's website.

References
Anderson JS, Parker RP (1998). The 3' to 5' degradation of yeast mRNAs is a general mechanism for mRNA turnover that requires the SKI2 DEVH box protein and 3' to 5' exonucleases of the exosome complex. *EMBO J.* doi:10.1093/emboj/17.5.1497

Bazzini, A. A., Del Viso, F., Moreno-Mateos, M. A., Johnstone, T. G., Vejnar, C. E., Qin, Y., . . . Giraldez, A. J. (2016). Codon identity regulates mRNA stability and translation efficiency during the maternal-to-zygotic transition. *The EMBO journal*. doi:10.15252/embj.201694699

Boël G., Letso R., Neely R., Price W. N., Wong K., Su M., Luff J. D., Valecha M., Everett J. K., Acton T. B., Xiao R., Montelione G. T., Aalberts D. P., Hunt J. F. (2016). Codon influence on protein expression inE. coli correlates with mRNA levels. *Nature*. doi:10.1038/nature16509

Burow D. A., Martin S., Quail J. F., Alhusaini N., Coller J., Cleary M. D. (2018). Attenuated Codon Optimality Contributes to Neural-Specific mRNA Decay in Drosophila. *Cell Reports*. doi:j.celrep.2018.07.039

Buschauer, R., Matsuo, Y., Sugiyama, T., Chen, Y.-H., Alhusaini, N., Sweet, T., . . . Beckmann, R. (17 de 04 de 2020). The CCR4-NOT complex monitors the translating ribosome for codon optimality. *Science*.

Carneiro, R. L., Requião, R. D., Rossetto, S., Domitrovic, T., & Palhano, F. L. (2019). Codon stabilization coefficient as a metric to gain insights into mRNA stability and codon bias and their relationships with translation. *Nucleic Acids Research*. doi: 10.1093/nar/gkz033

Collart M. A. 2016. The Ccr4-Not complex is a key regulator of eukaryotic gene expression. *WIREs RNA*. Doi:10.1002/wrna.1332

dos Reis, M., Savva, R., & Wernisch, L. (2004). Solving the riddle of codon usage preferences: a test for translational selection. *Nucleic Acids Research*. doi:10.1093/nar/gkh834

Dowdle, M. E., & Lykke-Andersen, J. (2025). Cytoplasmic mRNA decay and quality control machineries in eukaryotes. *Nat Rev Genet*. doi:10.1038/s41576-024-00810-1

Drummond, D. A., & Wilke, C. O. (2008). Mistranslation-induced protein misfolding as a dominant constraint on coding-sequence evolution. *Cell*. doi:10.1016/j.cell.2008.05.042

Du H., Zhao Y., He J., Zhang Y., Xi H., Liu M., Ma J., Wu L. (2016). YTHDF2 destabilizes m6A-containing RNA through direct recruitment of CCR4-NOT deadenylase complex. *Nature Communications*. doi:10.1038/ncomms12626

Enwerem I. I. I., Elrod N. D., Chang C., Lin A., Ji P., Bohn J. A., Levdansky Y., Wagner E. J., Valkov E., Goldstrohm A. C. (2021) Human Pumilio proteins directly bind the CCR4-NOT deadenylase complex to regulate the transcriptome. *RNA*. doi:10.1261/rna.078436.120

Forrest, M. E., Pinkard, O., Martin, S., Sweet, T. J., Hanson, G., & Coller, J. (2020). Codon and amino acid content are associated with mRNA stability in mammalian cells. *PLOS One*. doi: 10.1371/journal.pone.0228730

Frischmeyer, P. A., Hoof, A. V., O'Donnell, K., Guerrerio, A. L., Parker, R., & Dietz, H. C. (2002). An mRNA surveillance mechanism that eliminates transcripts lacking termination codons. *Science*. doi:10.1126/science.1067338

Gustafsson, C., Govindarajan, S., & Minshull, J. (2004). Codon bias and heterologous protein expression. *Trends in Biotechnology*. doi: 10.1016/j.tibtech.2004.04.006

Hosoda N., Funakoshi Y., Hirasawa M., Yamagishi R., Asano Y., Miyagawa R., Ogami K., Tsujimoto M., Hoshino S. (2011). Anti-proliferative protein Tob negatively regulates CPEB3 target by recruiting Caf1 deadenylase. *EMBO J*. doi:10.1038/emboj.2011.37

Hwang, S. S., Lim, J., Yu, Z., Kong, P., Sefik, E., Xu, H., . . . Flavel, R. A. (2020). mRNA destabilization by BTG1 and BTG2 maintains T cell quiescence. *Science*. doi: 10.1126/science.aax0194

Jeacock L., Faria J., Horn D. (2018). Codon usage bias control mRNA and protein abundance in trypanosomatids. *Elife*. doi:10.7554/eLife.32496

Jinek M, Coyle SM, Doudna JA. (2011). Coupled 5′ nucleotide recognition and processivity in Xrn1-mediated mRNA decay. *Mol Cell*. doi:10.1016/j.molcel.2011.02.004

Johnson AW, Kolodner RD. (1995). Synthetic lethality of sep1 (xrn1) ski2 and sep1 (xrn1) ski3 mutants of Saccharomyces cerevisiae is independent of killer virus and suggests a general role for these genes in translation control. *Mol Cell Biol.* doi:10.1128/MCB.15.5.2719

Klauer, A. A., & Hoof, A. v. (2012). Degradation of mRNAs that lack a stop codon: a decade of nonstop progress. *Wiley Intediscip Rev RNA*. doi: 10.1002/wrna.1124

McGlincy N. J., Ingolia N. T. (2017), Transcriptome-wide measurement of translation by ribosome profiling. *Methods*. doi:10.1016/j.ymeth.2017.05.028

Mishima, Y., & Tomari, Y. (2016). Codon Usage and 3' UTR Length Determine Maternal mRNA Stability in Zebrafish. *Mol Cell*. doi:10.1016/j.molcel.2016.02.027

Narula, A., Ellis, J., Taliaferro, J. M., & Rissland, O. S. (2019). Coding regions affect mRNA stability in human cells. *RNA*. doi:10.1261/rna.073239.119

Nascimento J. F., Kelly S., Sunter J., Carrington J. (2018). Codon choice directs constitutive mRNA levels in trypanosomes. *Elife*. doi:10.7554/eLife.32467

Ogami K., Hosoda N., Funakoshi Y., Hoshino S. (2014). Antiproliferative protein Tob directly regualtes c-myc proto-oncogene expression through cytoplasmic polyadenylation element-binding protein CPEB. *Oncogene*. doi:onc.2012.548

Passmore LA, Coller J. (2022). Roles of mRNA poly(A) tails in regulation of eukaryotic gene expression. *Nat Rev Mol Cell Biol* doi:10.1038/s41580-021-00417-y

Presnyak, V., Alhusaini, N., Chen, Y.-H., Martin, S., Morris, N., Kline, N., . . . Coller, J. (2015). Codon Optimality is a major determinant of mRNA stability. *Cell*. doi:10.1016/j.cell.2015.02.029

Radhakrishnan, A., Chen, Y.-H., Martin, S., Alhusaini, N., Green, R., & Coller, J. (2016). The DEAD-Box protein Dhh1p couples mRNA decay and translation by monitoring codon optimality. *Cell*. doi:10.1016/j.cell.2016.08.053

Raisch T., Valkov E. (2022). Regulation of the multisubunit CCR4-NOT deadenylase in the initiation of mRNA degradation. *Current Opinion in Structural Biology*. doi:10.1016/j.sbi.2022.102460

Webster, M. W., Chen, Y.-H., Stowell, J. A., Alhusaini, N., Sweet, T., Graveley, B. R., . . . Passmore, L. A. (2018). mRNA Deadenylation is coupled to translation rates by the differential activities of CCR4-NOT nucleases. *Mol Cell*. doi: 10.1016/j.molcel.2018.05.033

Wolf J, Passmore LA. (2014). mRNA deadenylation by Pan2–Pan3. *Biochem Soc Trans*. doi:10.1042/BST20130211

Wu Q., Medina S. G., Kushawah G., DeVore M. L., Castellano L. A., Hand J. M., Wright M., Bazzini A. A. (2019). Translation affects mRNA stability in a codon-dependent manner in human cells. *Elife*. doi:10.7554/eLife.45396

Wurtmann, E. J., & Wolin, S. L. (2009). RNA under attack: Cellular handling of RNA damage. *Crit Rev Biochem Mol Biol*. doi:10.1080/10409230802594043

Yan, L. L., Simms, C. L., McLoughlin, F., Vierstra, R. D., & Zaher, H. S. (2019). Oxidation and alkylation stresses activate ribosome-quality control. *Nat Commun*. doi:10.1038/s41467-019-13579-3

Yi H., Park J., Ha M., Lim J., Chang H., Kim V. N. (2018). PABP Cooperates with the CCR4-NOT Complex to Promote mRNA Deadenylation and Block Precocious Decay. *Mol Cell*. doi:10.1016/j.molcel.2018.05.009

Yu, C., Ji, S.-Y., Sha, Q.-Q., Dang, Y., Zhou, J.-J., Zhang, Y.-L., . . . Fan, H.-Y. (2016). BTG4 is a meiotic cell cycle-coupled maternal-zygotic-transition licensing factor in oocytes. *Nat Struct Mol Biol*. doi:10.1038/nsmb.3204

Zhu, X., Cruz, V. E., Zhang, H., Erzberger, J. P., & Mendell, J. T. (2024). Specific tRNAs promote mRNA decay by recruiting the CCR4-NOT complex to translating ribosomes. *Science*. doi: 10.1126/science.adq8587